



ELSEVIER

Contents lists available at ScienceDirect

Journal of Magnetism and Magnetic Materials

journal homepage: www.elsevier.com/locate/jmmm

Effects of processed parameters on the magnetic performance of a powder magnetic core

Ding-Zhou Xie^a, Kuan-Hong Lin^{b,*}, Shun-Tian Lin^a^a Department of Mechanical Engineering, National Taiwan University of Science and Technology, Taipei 106, Taiwan, ROC^b Department of Mechanical Engineering, Tunghan University, New Taipei City 222, Taiwan, ROC

ARTICLE INFO

Article history:

Received 13 June 2013

Received in revised form

24 September 2013

Available online 22 October 2013

Keywords:

Magnetic core

Phosphate treatment

Iron loss

Eddy current loss

Hysteresis loss

ABSTRACT

The goal of this study is to develop a high magnetic flux density and low iron loss powder magnetic core with insulated layer coating on pure iron powders of varying sizes. After processing the phosphate treatment, the insulated layer $Zn_3(PO_4)_2$ was coated onto the iron powder surface. It not only maintained the magnetic flux density of pure iron, but also enhanced the electrical resistivity of the magnetic core by reducing eddy current loss, which allowed a wider frequency range. In addition, the annealing treatment after the compression process raised the magnetic flux density of the magnetic core; however, an annealing temperature above 200 °C caused the binder to decompose, resulting in decreased electrical resistivity. Experimental results indicate that the best magnetic performances were achieved with a powder magnetic core of fine and coarse iron powder proportion of 2:1, phosphate treatment of 90 s, and an annealing temperature of 200 °C.

© 2013 Elsevier B.V. All rights reserved.

1. Introduction

Soft magnetic material is widely used in alternating current (AC) magnetic field applications, due to its high saturation magnetic flux density, high permeability, low coercive force at a low magnetic field, as well as low energy loss at the AC magnetic field [1–3].

Three categories of soft magnetic materials are well known. The first is a sintered Fe-based alloy that is commonly added of various alloys to enhance magnetic performance. Some examples of these are Fe, Fe–Si, Fe–P, Fe–Ni, and Fe–Co alloys [4–6]. Sintered Fe-based alloys are known for their high saturation magnetic flux density and effective permeability at low frequencies. Nevertheless, they demonstrate a high iron loss and energy loss at high frequencies because of their low electrical resistance. The sintered Fe-based alloy magnetic core is used as an electromagnetic conversion component in transformers and motors [4–6]. The second category is ferrite, which includes NiO, Fe_2O_3 , MnO, Fe_2O_3 , and CuO, Fe_2O_3 , and has a high electrical resistance at high frequencies [2,7–9]. The saturation magnetic flux density and permeability of ferrite is lower than that of sintered Fe-based alloy. Accordingly, ferrite magnetic cores are suitable only for low-power applications such as a medium-to-high frequency transformer, radio, and wave filter components [7–9].

The third category is the powder magnetic core, which is fabricated by powder metallurgy. It is a compact body of iron

powders individually covered with an insulation layer, classified as a soft magnetic composite (SMC) [10–11]. The powder magnetic core has a high magnetic flux density, permeability, and electrical resistance; accordingly, it reduces iron loss at high-frequency bands. It is normally used as the inductor and wave filter component with operating frequencies ranging from 100 Hz to 300 kHz [11–13]. The electrical resistivity of pure iron at 20 °C is only $10^{-7} \Omega m$, thus it causes a higher energy loss for power conversion systems [14]. Therefore, the insulation layer is coated on the iron powder surface to increase the resistivity of a magnetic core. The insulation layer most commonly coated on the iron powder is magnesium oxide and phosphate glass [3,15–16]. The magnesium oxide insulation coating has greater heat resistance, lower electrical resistivity ($2.1 \times 10^{-5} \Omega m$), and lower iron loss than the conventional phosphate insulation coating [3,17].

Phosphate insulation coating is commonly applied to conventional SMCs because of its properties of high electrical resistivity (over $5 \times 10^{-5} \Omega m$), permeability, saturation magnetic flux density, and firm adhesiveness to iron powder; furthermore, it can be fabricated easily [13,15–16]. In this study, phosphate insulation coating was applied to the surface of iron powder to increase electrical resistivity. A powder magnetic core with high magnetic flux density, high permeability, and low energy loss at high frequencies was expected.

2. Experimental procedures

The basal powders used in this study were carbonyl iron powder and water-atomized iron powder (Yuelong Metal Powder Co., Ltd)

* Corresponding author. Tel.: +886 2 86625917; fax: +886 2 86625919.

E-mail addresses: khlin@mail.tnu.edu.tw, lk1805@gmail.com (K.-H. Lin).

with an average particle size of 6.5 μm and 45 μm , and carbon content of 0.46 wt% and 0.004 wt%, respectively. Fig. 1(a) and (b) show particle size analysis results of carbonyl iron powder and water-atomized iron powder, respectively. The phosphate treatment was executed by mixing the iron powders with a zinc phosphate solution (Tanmax Coating, zinc phosphate #838) at room temperature for 90 s, 50 s and 0 s, respectively. The powders were then rinsed in water for 30 min to remove impurities, and then heated to dry. Subsequently, these powders were mixed, according to the percentages listed in Table 1. Following phosphate conversion coating, the powders were blended with a solution containing 12.64 vol% bakelite (K.L. Chemicals, RA8816HP) for 24 h and then granulated by spray drying. A pressure of 330 MPa was applied to a cylindrical die to fabricate a ring-shaped specimen with an outer diameter of 10 mm, internal diameter of 3.2 mm, and a thickness of 4 mm. The compacted specimen was then hardened at 150 $^{\circ}\text{C}$ and annealed in argon atmosphere at 200 $^{\circ}\text{C}$, 300 $^{\circ}\text{C}$, and 400 $^{\circ}\text{C}$ for 30 min, respectively.

Secondary electron images (SEI) of the iron powder and phosphate coated layer were recorded using a scanning electron microscope (SEM, JEOL, JSM-T330A). The crystalline structure of the phosphate layer of iron powder was analyzed using an X-ray diffractometer (XRD, REGAKU, DMAX-VB) at 40 kV and 100 mA, using CuK_{α} ($\lambda=0.15418$ nm) radiation.

To evaluate magnetic performance, a vibrating sample magnetometer (VSM, LAKE SHORE, 730 M) was used to record the hysteresis curve and coercive force of a powder magnetic core (ring-shaped specimen given 15 turns of coil winding) at room temperature and direct current (DC) condition. The maximum field was set to 7 kOe, the field increment was 282.02 Oe and, the average time for each point was 3 s. The initial permeability and permeability at magnetic flux density 10 kG, and iron-loss of a powder magnetic core were measured with an AC B - H curve tracer (IWATSU, SY-8258). The electrical resistance (R) of the powder magnetic core was measured with a 4-point probe, and then converted into electrical resistivity (ρ) by the equation: $\rho=R \times A/l$.

3. Results and discussion

3.1. Microstructure

Fig. 2(a) and (b) show secondary electron images of the original water-atomized iron powders (average particle size 45 μm) and those after 90 s of phosphate treatment, respectively. Fig. 2(c) and (d) show secondary electron images of the original carbonyl iron powders (average particle size 6.5 μm) and those after 90 s of phosphate treatment, respectively. As shown in Fig. 2(b), a large quantity of compact acicular lamellae accumulated on the surface. Regarding the carbonyl iron powder, the compact acicular lamellas were not obvious on the surface (Fig. 2(d)). Fig. 3(a) and (b) show optical photomicrographs of the specimens A1 and A2, respectively.

Fig. 4 shows the X-ray diffraction (XRD) pattern of the water-atomized iron powders after 90 s of phosphate treatment. The Miller indices corresponding to each peak in the diffraction pattern demonstrate a specific set of planes in the $\text{Zn}_3(\text{PO}_4)_2$ phase. Therefore, the acicular lamellae coated on the iron powder surface is $\text{Zn}_3(\text{PO}_4)_2$ with a monoclinic crystal structure (JCPDS 30-1490).

3.2. Effect of coarse and fine iron powder on magnetic performance

Table 2 shows the resistivity of five powder magnetic cores (A1 to A5) fabricated with various percentages of water-atomized iron powder (coarse powder) and carbonyl iron powder (fine powder). Powder magnetic core A1, which is composed of the highest percentage of coarse powder, had the lowest resistivity. Previous research indicated that a powder magnetic core fabricated with larger iron powders had a higher saturation magnetic flux density and permeability, but also a higher iron-loss due to the lower resistivity of the coarse iron powder [1,18]. For this reason, two iron powders of different sizes were mixed together to fabricate the powder magnetic core in this study. The powder magnetic core was expected to maintain a high saturation magnetic flux density and high permeability, as well as increase resistivity to reduce iron-loss.

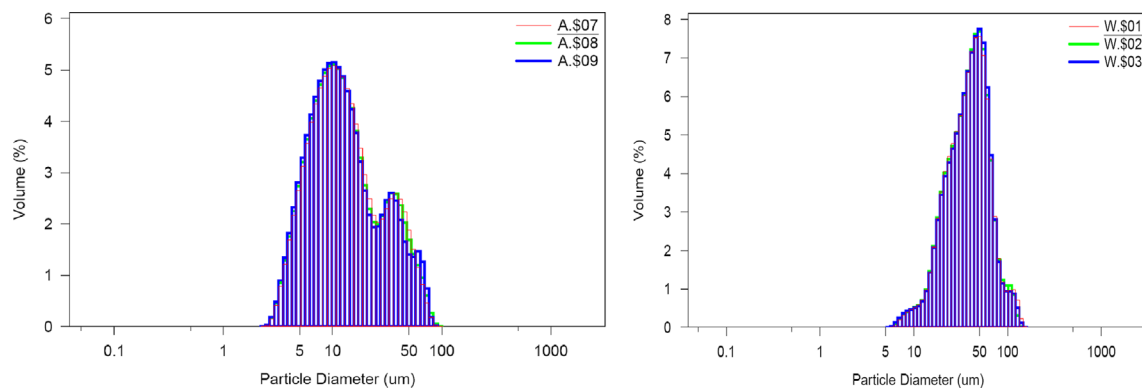


Fig. 1. Particle size analysis results: (a) carbonyl iron powder and (b) water-atomized iron powder.

Table 1

Designation and process parameters of specimens.

Specimen designation	A1	A2	A3	A4	A5	B1	B2	C1	C2
6.5 μm iron powder (wt%)	50	66.7	75	80	83.3	66.7	66.7	66.7	66.7
45 μm iron powder (wt%)	50	33.3	25	20	16.7	33.3	33.3	33.3	33.3
Phosphate treatment (s)	90	90	90	90	90	50	0	90	90
Annealing temperature ($^{\circ}\text{C}$)	200	200	200	200	200	200	200	300	400

Download English Version:

<https://daneshyari.com/en/article/8157451>

Download Persian Version:

<https://daneshyari.com/article/8157451>

[Daneshyari.com](https://daneshyari.com)